Inhibition of Copper Corrosion in NaCl Solution by Caffeic Acid

L. Vrsalović[1,], S. Gudić[1], M. Kliškić[1], E. E. Oguzie[2], L. Carev[1]*

[1]Department of Electrochemistry and Materials Protection, Faculty of Chemistry and Technology, Split, Croatia
[2]Electrochemistry and Materials Science Research Laboratory, Department of Chemistry, Federal University of Technology Owerri, Owerri, Nigeria
[*]E-mail: ladislav@ktf-split.hr

The inhibition of copper corrosion by caffeic acid in 10 % ethanolic 0.5 M NaCl solution was assessed using different electrochemical and computational. Results of investigations showed that caffeic acid inhibited copper corrosion in the studied environment via adsorption on the Cu/corrodent interface. The compound essentially functioned as a cathodic inhibitor for copper corrosion and the inhibition efficiency increased with concentration. The adsorption behavior of caffeic acid on the Cu electrode surface followed the Freundlich adsorption isotherm with the free energy of adsorption $\Delta G = -10.922$ kJ mol^{-1}, which indicates physical adsorption. Molecular-level insight into the adsorption behavior was achieved via quantum chemical computations to ascertain the electronic structure of the molecule and molecular dynamics simulations to probe the interaction of the molecule with the Cu surface. The models corroborated the experimental results.

1. INTRODUCTION

Copper is known to possess exceptional electrical and thermal conductivity, combined with good mechanical workability, as well as superior corrosion resistance in non-oxidizing solutions, making it one of the most widely used metallic materials [1]. However in the presence of complexing ions, such as Cl$^-$, copper may suffer severe corrosion, so it is necessary to use some method for corrosion protection in such environments. Although there are different corrosion control methods available [2,3], corrosion protection in fluid environments is more appropriately achieved using

corrosion inhibitors. These days, compounds derived from natural products have been found to exhibit strong affinity for corroding metal surfaces and are attracting lots of attention in the search for benign corrosion inhibitors [4-8].

Caffeic acid is a phenolic acid found in plants like carrot, tomato, strawberry, and blueberry and is among the major hydroxycinnamic acids present in wine [9-11]. Structural formula of caffeic acid is shown on Fig 1.
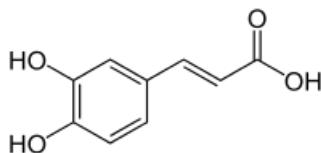

Figure 1. Chemical structure of caffeic acid

Caffeic acid and its derivatives continue to attract considerable attention due to their biological and pharmacological activities, including antioxidative activities, anti-inflammatory activities, etc [11-13].

Previous studies have revealed that phenolic acids inhibit the corrosion of Al-Mg alloys [14,15], CuNiFe alloy [16] and steel [17]. On the other hand, there are only few reports on the corrosion inhibition performance of caffeic acid in the literature. Pirvu and associates highlighted the potential use of some vegetal extracts containing high quantities of caffeic acid derivates, which show considerable corrosion inhibiting efficacy [18,19]. De Sousa and Spinelli [30] reported that caffeic acid inhibited corrosion of mild steel in 0.1 M H_2SO_4 solution. Corrosion inhibition of iron and aluminum by caffeic acid and other bio-organic compounds have been studied by McCafferty and Hansen [21]. Improvement of the corrosion resistance of mild steel in cooling water systems by addition of poly (acrylate-co-caffeic acid) and other acrylate–caffeic copolymers was reported by Sekine and co-workers [23]. Other environmentally safe polyphenol polymers have also been assessed as corrosion inhibitors under alkaline conditions in boiler systems [24].

The present study evaluates the corrosion inhibition action of caffeic acid on copper corrosion in 10 % ethanolic 0.5 M NaCl solution using combined experimental and computational techniques. Test variables have been adjusted in order to enable sufficient information on the mechanism the corrosion inhibition process.

2. EXPERIMENTAL

2.1. Materials Preparation

Copper electrode in the form of a cylinderical rod of 0.6 cm diameter and purity 99.98% was used for polarization and electrochemical impedance spectroscopy measurements. The lateral section of working electrode was insulated with Polyrepair resin, leaving an area 0.282 cm^2 exposed. Before each measurement electrode surface was abraded with emery paper to a 1500 metallographic finish and finally rinsed ultrasonically in deionized water and ethanol.

Caffeic acid (97%) and the NaCl (99%) were acquired from Aldrich. Solution was prepared as 10 % ethanolic solution to enhance the limited solubility of caffeic acid. Solution pH was adjusted to 5.5 using 0.1 M NaOH solution.

2.2. Electrochemical Experiments

For electrochemical measurements, EG&G potentiostat/galvanostat Model 273A in combination with a lock-in amplifier (PAR M5210) was employed. The reference electrode was a saturated calomel electrode (SCE), while the counter electrode was a Pt plate. All potentials are reported vs. SCE. Experiments were performed using electrodes immersed for 1 h in the different test solutions. Polarization measurements were controlled with PARC corrosion analysis software M 352/252 SoftCorr. Linear polarization measurements were performed in the range of ±20 mV vs. E_{corr}. Potentiodynamic polarization measurements were performed with potential scan from the most negative potentials (-200 mV vs. E_{corr}) up to the +350 mV vs. E_{corr} with the scan rate of 0.2 mV s^{-1}. Electrochemical impedance measurements were controlled with Power Sine software. Impedance measurements were carried out at E_{corr}, with a signal amplitude perturbation of 10 mV and frequency range 50 kHz - 30 mHz. Electrochemical experiments were undertaken in the temperature range 30 – 50 ^{o}C.

2.3. Computational Studies

Materials Studio 4.0 software was employed for the computational studies, using the electronic structure programs Forcite and DMol 3.

3. RESULTS AND DISCUSSION

3.1. Open circuit potential measurements

The influence of caffeic acid concentration on the evolution of Cu open circuit potential (E_{OC}) in 10 % ethanolic 0.5 M NaCl was studied at 20 ^{o}C and the obtained results presented in Fig. 2. The plots reveal two distinct trends; a steep negative displacement of potential for all systems during the initial periods of immersion, due possibly to dissolution of the air-formed surface oxide layer in the test solution. The potential stabilized thereafter, maintaining relatively stable values. Similar observation was reported in [25-27].
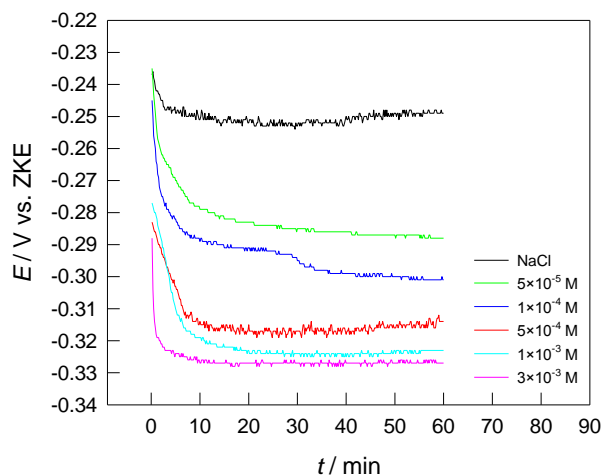
Figure 2. Effect of caffeic acid on the evolution of open circuit potential for Cu in 10% ethanolic 0.5 M NaCl at 20 ^{o}C.

It is as well obvious that caffeic acid modified the E_{OC} values with the highest concentration of caffeic acid (0.03 M) exerting the most pronounced effect. The change in the E_{OC} values with the addition of inhibitor is often a useful indication of which reaction is more affected: cathodic or anodic. Under the presence of caffeic acid in NaCl solution E_{OC} shifts to more negative values and the magnitude of such shifts increases with caffeic acid concentration. These results suggest that caffeic acid would exert a predominant cathodic effect in inhibiting copper corrosion in 10 % ethanolic 0.5 M NaCl [26].

3.2. Polarization measurements

Linear polarization measurements were performed in order to determine the influence of caffeic acid on the polarization resistance of copper in 10 % ethanolic 0.5 M NaCl. Results of these investigations at 20 ^{o}C are shown in Fig 3.
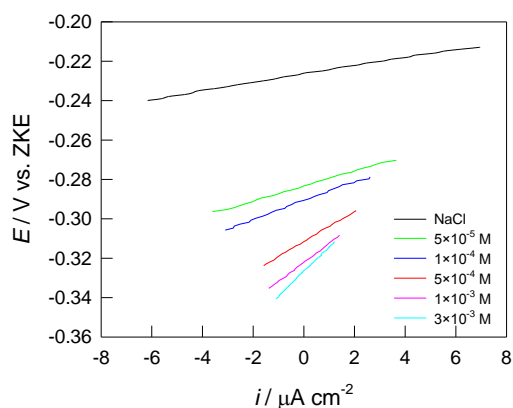

Figure 3. Linear polarization curves for Cu in 10% ethanolic 0.5 M NaCl containing caffeic acid at 20 ^{o}C

Polarization resistance values were obtained form the slopes of the polarization curves in the vicinity of E_{corr} (±10 mV from E_{corr}). From the R_p values, the surface coverage (θ), and the inhibition efficiency (η%) were calculated using the equations:

$$\theta = \left(\frac{R_{pi} - R_p}{R_{pi}} \right) \tag{1}$$

$$\eta\% = \theta \times 100 \tag{2}$$

where R_p is the polarization resistance in uninhibited solution and R_{pi} the polarization resistance in the presence of caffeic acid. The values of the linear polarization parameters are shown in Table 1:

Table 1. Linear polarization parameters for copper corrosion in ethanolic 0.5 M NaCl, without and with different concentrations of caffeic acid at different temperatures

c mol dm^{-3}	R_p kΩ cm^2	θ	η%
T = 20 ^{o}C			
0	2.111	-	-
5×10^{-5}	3.854	0.4510	45.10
1×10^{-4}	4.797	0.5600	56.00
5×10^{-4}	7.589	0.6955	69.55
1×10^{-3}	9.599	0.7801	78.01
3×10^{-3}	13.462	0.8432	84.32
T = 30 ^{o}C			
0	1.562		
1×10^{-3}	6.101	0.7440	74.40
T = 40 ^{o}C			
0	1.134		
1×10^{-3}	3.757	0.6981	69.81
T = 50 ^{o}C			
0	0.620		
1×10^{-3}	1.655	0.6254	62.54

It can be seen that R_p values increased with caffeic acid concentration, but decreased with rise in temperature. The same trend is reflected in the values of surface coverage and inhibition efficiency.

Potentiodynamic polarization curves were recorded to obtain information about the influence of caffeic acid on anodic and cathodic processes on copper corrosion in the test solution [25, 26]. Representative potentiodynamic polarization curves are presented in Figure 4.
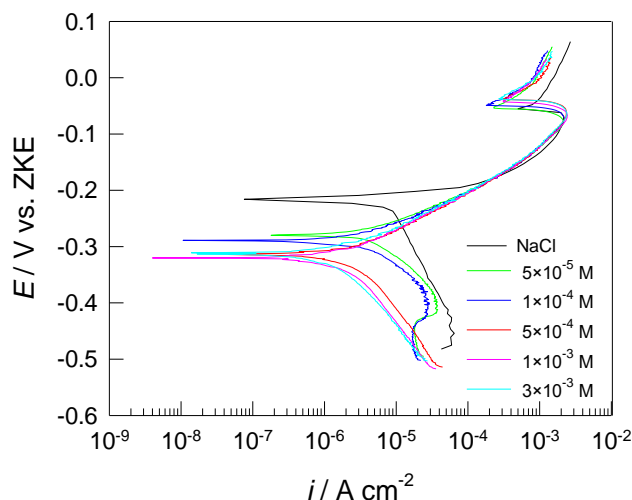
Figure 4. Potentiodinamic polarization curves for Cu in 10 % ethanolic 0.5M NaCl containing different concentration of caffeic acid at 20 °C.

Table 2. Potentiodynamic polarization parameters for Cu in 10 % ethanolic 0.5 M NaCl with caffeic acid

c mol dm^{-3}	b_c V dec^{-1}	b_a V dec^{-1}	i_{corr} μA cm^{-2}	E_{corr} V	θ	η %
			T = 20 °C			
0	-0.230	0.034	8.75	-0.216	-	-
5×10^{-5}	-0.110	0.060	4.40	-0.280	0.4966	49.66
1×10^{-4}	-0.110	0.065	3.90	-0.289	0.5540	55.40
5×10^{-4}	-0.156	0.064	2.88	-0.314	0.6703	67.03
1×10^{-3}	-0.162	0.063	2.18	-0.320	0.7512	75.12
3×10^{-3}	-0.150	0.064	1.40	-0.313	0.8400	84.00
			T = 30 °C			
0	-0.154	0.059	12.5	-0.278	-	-
1×10^{-3}	-0.173	0.063	3.4	-0.295	0.728	72.80
			T = 40 °C			
0	-0.147	0.062	15.6	-0.296	-	-
1×10^{-3}	-0.200	0.061	4.89	-0.296	0.6865	68.65
			T = 40 °C			
0	-0.284	0.066	23.8	-0.305	-	-
1×10^{-3}	-0.276	0.070	9	-0.298	0.6218	62.18

The potentiodynamic polarization results show clearly that increasing caffeic acid concentrations caused the cathodic polarization curves to be shifted towards lower current densities and the corrosion potential shifted toward more negative values. This implies that caffeic acid almost selectively inhibited the cathodic reaction [26], thus corroborating the findings from the open circuit potential measurements. Corrosion parameters derived from the potentiodynamic polarization curves are presented in the Table 2, along with the values of surface coverage and the inhibition efficiency ($\eta\% = 100 \times \theta$) calculated from equation 3.

$$\theta = \frac{i_{corr} - (i_{corr})_i}{i_{corr}} \qquad (3)$$

i_{corr} and $(i_{corr})_i$ are the values of corrosion current density without and with caffeic acid. From the Table 2 it can be seen that the efficiency of the caffeic acid again increased with concentration but decreased with increase in system temperature.

3.3. Impedance measurements

The primary objective of the impedance measurements was to better understand the processes taking place at the copper/solution interphase and how caffeic acid modified such processes [25, 26]. Figure 5 shows Bode representations of the impedance responses for the Cu electrode in 10 % ethanolic 0.5M NaCl, i.e. plots of logarithm of impedance, Z, and phase angle respectively *vs.* logarithm of frequency, *f* in the absence and presence of caffeic acid. In the high frequency region (*f* > 1 kHz), the log |Z| values are low, tending towards constant values, while phase angle values fall rapidly towards 0°. This is a classic resistive response, corresponding to the electrolyte resistance. In the mid frequency region, the linear relationship between log |Z| and log *f*, with slope tending towards -1 and phase angle about -70° mirror the capacitive behavior of the system. At low frequency, the -40° phase angle and log |Z| *vs.* log *f* (-0.5) slope all point towards a slow diffusion process. It is obvious that the total impedance of the system increased with caffeic acid concentration, implying that the electrode surface was more protected. Similar observations have been reported elsewhere for other corrosion inhibitors [27-32].
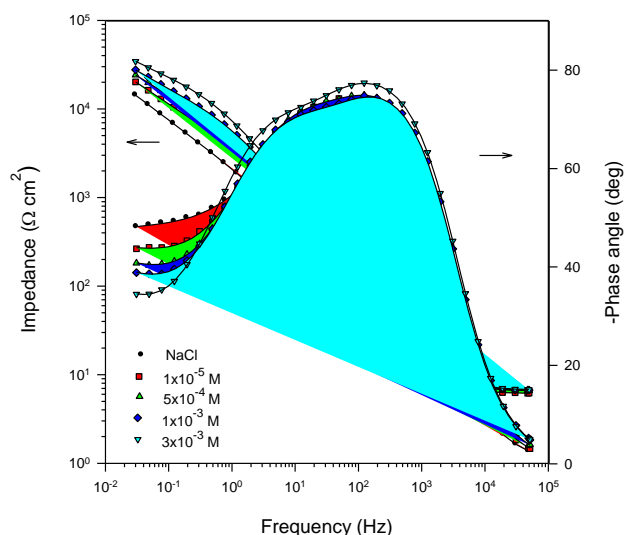

Figure 5. Bode plots for Cu in 10 % ethanolic 0.5 M NaCl containing caffeic acid

The appearance of more than one time constant in the impedance spectra reflects the diversity of the interfacial phenomena in the systems under investigation [25]. The equivalent circuit proposed

to fit the experimental data is shown in Figure 6 and has been previously used to describe the impedance response of Cu in chloride media [33]. The circuit consists of an electrolyte resistance R_{el} ($\approx 5 \ \Omega \ cm^2$) associated with two time constants. The initial time constant at high frequencies often results from the rapid charge transfer processes associated with the metal (copper) dissolution process; R_1 represents the charge transfer resistance, and Q_1 represents the constant phase element and replaces the capacitance of the electrical double layer [25, 33]. Added equivalent circuit parameters were introduced to account for the corrosion product surface layer and diffusion process at low frequencies, such as R_2 for the surface layer resistance, Q_2 for constant phase element of the surface layer (Q_2 replaces the capacitance of surface layer) and a Warburg impedance W for the diffusion process [33].
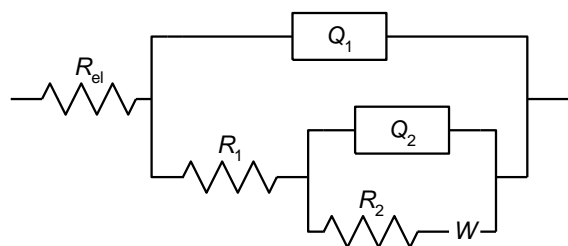

Figure 6. Equivalent circuit for modeling the impedance response of Cu in 10 % ethanolic 0.5 M NaCl

A constant phase element is used to replace the capacitive elements in either time constant of the equivalent circuit. Such a CPE is introduced to accommodate deviations from ideal capacitive response connected with depression of capacitive loops in Nyquist plots. The CPE's impedance (Z_{CPE}) corresponds to [34, 35]:

$$Z_{CPE} = \left[Q(j\omega)^n \right]^{-1} \tag{4}$$

wherein $-1 \leq n \leq 1$, $j = \sqrt{-1}$ and $\omega = 2\pi f$, whereas Q is a frequency-independent constant, having the features of pure capacitance when $n = 1$; resistance when $n = 0$; inductance when $n = -1$; while diffusion processes are characterized by $n = 0.5$.

Table 3. Impedance parameters for the Cu in 10 % ethanolic 0.5 M NaCl containing caffeic acid

c (mol dm^{-3})	$Q_1 \times 10^6$ (Ω^{-1} s^n cm^{-2})	n_1	R_1 (kΩ cm^2)	$Q_2 \times 10^6$ (Ω^{-1} s^n cm^{-2})	n_2	R_2 (kΩ cm^2)	$W \times 10^4$ (Ω^{-1} s$^{0.5}$ cm^{-2})	$\eta\%$
0	45.53	0.89	0.28	34.71	0.62	2.01	1.25	-
5×10^{-5}	34.86	0.91	0.57	28.43	0.68	4.06	1.13	50.88
1×10^{-4}	25.44	0.92	0.64	20.76	0.72	4.81	1.10	56.25
5×10^{-4}	19.85	0.92	0.96	15.15	0.75	7.29	1.03	70.83
1×10^{-3}	17.40	0.91	1.24	12.99	0.77	9.81	0.97	77.42
3×10^{-3}	14.84	0.92	2.51	10.67	0.78	16.09	0.93	88.84

The parameters derived from the equivalent circuit in Figure 6 are presented in Table 3. The results

show that increasing the caffeic acid concentration caused a corresponding increase the values of charge transfer resistance (R_1) and surface layer resistance (R_2), which signifies improvement of corrosion resistance, while the capacitance of both the double layer and surface layer (Q_1 and Q_2) as well as the diffusion element (W) decreased.

The observed decrease in Q_1 and Q_2 values on addition of caffeic acid provides valid experimental evidence of adsorption of caffeic acid on the corroding Cu surface. Such behavior has been associated [29, 32] with the plate capacitor model, where [$C = \varepsilon_o\varepsilon/d$]. ε_o is the permittivity of vacuum; and ε the relative permittivity of the film). Hence, the reduction of Q_2 with the increase of inhibitor concentration matches the corresponding increase in the thickness of the adsorbed inhibitor layer, which additionally corresponds to an enhancement in the protective properties of the inhibitor. The evolution correlates with the observed improvement of the quality of the inhibitor film, corresponding to enhanced charge transfer resistance. The values of n_2 associated with Q_2 are found in the 0.68–0.78 interval revealing that the adsorbed inhibitor layer was partially heterogeneous [28, 33]. On the other hand, the different values of n_2 are due to the modification of the structure of the adsorbed layer in combination with its thickness, as suggested by the R_2 values [33].
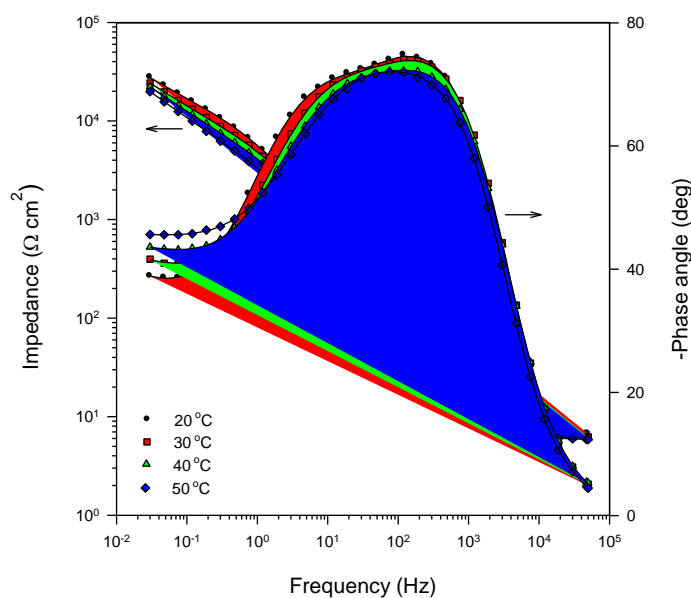

Figure 7. Bode plots for Cu in 10 % ethanolic 0.5 M NaCl with 1×10^{-3} mol dm^{-3} caffeic acid at different temperatures

The inhibition efficiency ($\eta\%$) can be then calculated from the charge transfer resistance values as follows:

$$\eta = \frac{(R_1)_{inh} - R_1}{(R_1)_{inh}} \times 100 \tag{5}$$

where R_1 and $(R_1)_{inh}$ are the charge transfer resistance without and with inhibitor, respectively. The obtained inhibition efficiency values for caffeic acid are given in Table 3. Inhibition efficiency increased with caffeic acid concentration, reaching maximum values of $\approx$ 85 %. The inhibition

efficiency determined from the polarization and impedance measurements are in a good correlation.

Effect of temperature on the impedance response of copper was investigated in 10% ethanol solution of NaCl in the presence of caffeic acid in concentration of 1×10^{-3} mol dm^{-3} at electrolyte temperatures of 20 °C, 30 °C, 40 °C and 50 °C. The obtained results are presented in a Figure 7 and Table 4:

Table 4. Effect of temperature on the impedance parameters for the Cu in 10 % ethanolic 0.5 M NaCl containing caffeic acid

t (°C)	$Q_1 \times 10^6$ (Ω^{-1} s^n cm^{-2})	n_1	R_1 (kΩ cm^2)	$Q_2 \times 10^6$ (Ω^{-1} s^n cm^{-2})	n_2	R_2 (kΩ cm^2)	$W \times 10^4$ (Ω^{-1} s$^{0.5}$ cm^{-2})
20	17.40	0.91	1.24	12.99	0.77	9.81	0.97
30	18.16	0.91	0.89	13.56	0.76	6.23	1.00
40	20.48	0.90	0.60	15.27	0.74	4.65	1.02
50	23.83	0.90	0.37	17.26	0.72	3.05	1.07

Increasing the temperature of the system caused the charge transfer resistance (R_1) and surface layer resistance (R_2) to decrease, while the capacitance of the double layer (Q_1), capacitance of the surface layer (Q_2) and the diffusion element (W) increased. This corresponds to an increase in copper dissolution rate and a reduction in the thickness of the adsorbed inhibitor. Both effects hindered the performance of caffeic acid at higher temperatures, leading to a decrease in inhibition efficiency with rise in temperature.

3.4 Adsorption models

Data obtained from potentiodynamic polarization measurements were fitted to various adsorption isotherm models. The best fit was obtained with the Freundlich model, which is represented by equation (6):

$$\theta = kC^n \qquad (6)$$

where c is inhibitor concentration, θ is surface coverage and K is adsorption constant. The equation can be linearized as shown in Eq. 7. From the linear dependence of ln θ vs. ln c, the adsorption constant can be determined from the intersection of line and y-axis.

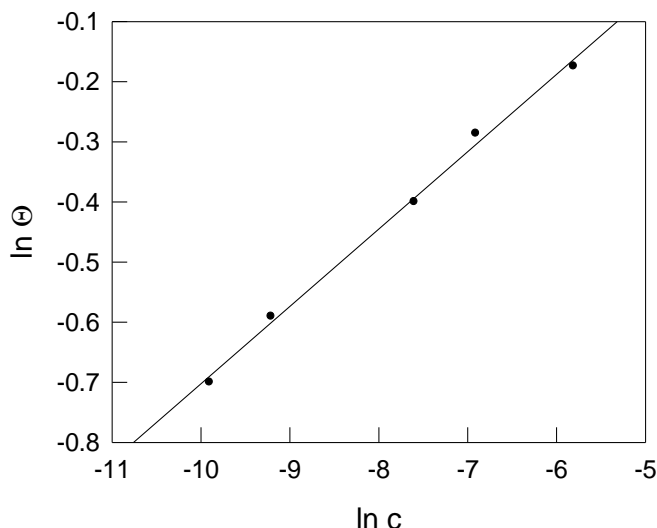$$\ln \theta = \ln k + n \ln C \qquad (7)$$

Figure 8. The Freundlich adsorption isotherm for caffeic acid onto a Cu surface in 10 % ethanolic 0.5 M NaCl

Fig 8 shows the Freundlich isotherm for caffeic acid adsorption on copper in 10 % ethanolic 0.5 M NaCl. The good linear fit of the plot as well as the r^2 value of 0.9961 confirms the data fit to the Freundlich isotherm. The equilibrium constant of adsorption is related to the standard energy of adsorption ΔG°_{ads} by:

$$K = \frac{1}{55.5} \exp\left(-\frac{\Delta G^{\circ}_{ads}}{RT}\right) \qquad (8)$$

The value of 55.5 is the concentration of water in the solution in mol dm^{-3}, R is the gas constant and T is the absolute temperature. The calculated standard energy of adsorption ΔG°_{ads} was -10.922 kJ mol^{-1}.

The negative values of ΔG°_{ads} indicate that the adsorption process proceeds spontaneously, and its value indicate that caffeic acid adsorb on copper by a physisorption-based mechanism. This mechanism is consistent with the observed decrease in inhibition performance with rise in temperature.

The dependence of the corrosion current on temperature can be regarded as an Arrhenius-type process, the rate of which is:

$$i_{corr} = A \exp\left(-\frac{E_a}{RT}\right) \qquad (9)$$

where i_{corr} is the corrosion current density, A is the Arrhenius preexponential constant and E_a is the apparent activation energy. Arhenius equation can be converting to a linear form:

$$\ln i = -\frac{E_a}{R} \cdot \frac{1}{T} + \ln A \qquad (10)$$

In this way it is possible to determine the value of activation energy from the slope of the linear plot, while the intercept on the Y-axes gives the value of the proportionality factor A. The corresponding Arrhenius plots for copper corrosion in absence and presence of caffeic acid are illustrated in Figure 9.
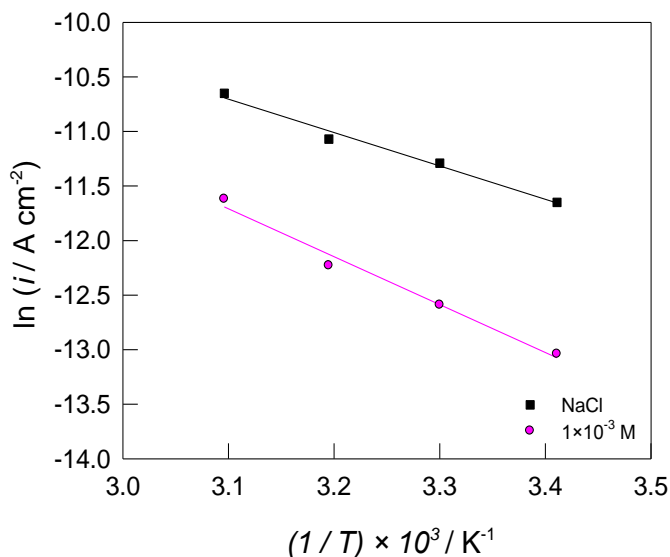
Figure 9. Arrhenius plots for Cu in 10 % ethanolic 0.5 M NaCl without and with caffeic acid in concentration 1×10^{-3} mol dm^{-3}.

Some conclusions about the mechanism of the inhibitor action can be obtained by comparing the E_a, values in the presence and absence of a corrosion inhibitor. Generally, if higher values of E_a are obtained in the presence of an inhibitor, compared to the uninhibited solution, physical adsorption mechanism can be inferred; conversely, lower E_a value obtained in the presence of inhibitor, compared to that in its absence indicate chemisorption of the corrosion inhibitor [4,35].

The E_a values determined from the slopes of the Arrhenius plots correspond to 25.45 kJ mol^{-1} in non-inhibited 10 % ethanolic 0.5 M NaCl and 36.48 kJ mol^{-1} in the presence of caffeic acid. The higher E_a value obtained in the presence of caffeic acid compared to that in its absence indicates physical adsorption of the corrosion inhibitor.

3.4. Computer simulation studies

Computational studies were undertaken to model those electronic properties of caffeic acid that could influence its adsorption, hence corrosion inhibition performance. Details of the computational protocol are presented elsewhere [36, 37]. The electronic properties of caffeic acid, including the optimized structure, total electron density, highest occupied and the lowest unoccupied molecular orbitals as well as Fukui functions are depicted in Fig. 10. The total electron density of the caffeic acid molecule (Fig. 10d) shows the charge distribution to be spread around the molecule, which should normally lead to a flat-lying adsorption orientation. Electrophiles often attack the regions of highest electron density, which denote the active centers, with the greatest capacity to bond to the metal surface. The HOMO energy (E_{HOMO}), reflects the tendency of a molecule to donate electrons, whereas the LUMO energy (E_{LUMO}) corresponds to a tendency for electron acceptance [38].
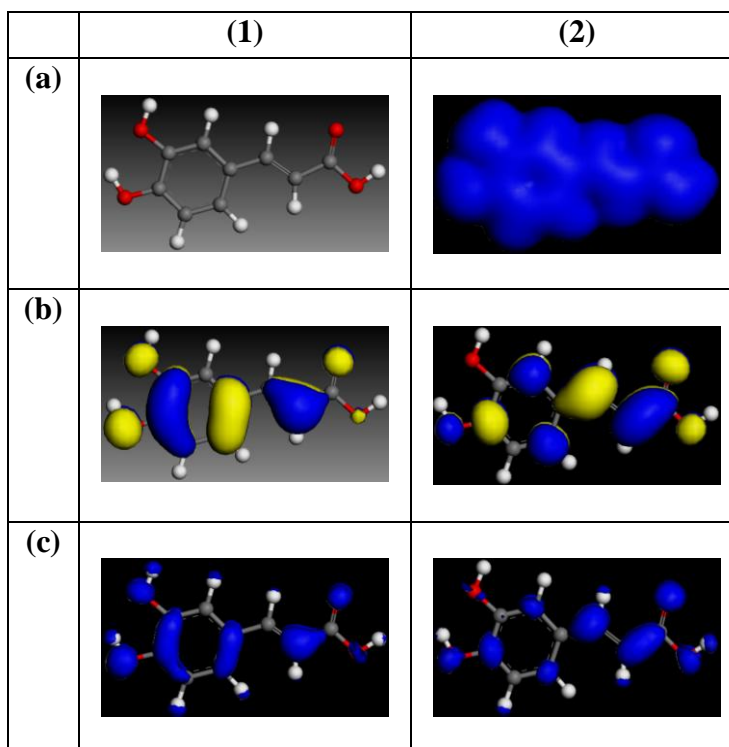
	(1)	**(2)**
(a)		
(b)		
(c)		

Figure 10. Electronic structures of caffeic acid: (a1) optimized structure, (a2) total electron density, (b1) HOMO orbital [E_{HOMO} = -5.35 eV], (b2) LUMO orbital [E_{LUMO} = -2.66 eV], (c1) Fukui f $^-$ function, (c2) Fukui f $^+$ function. Atom legend: white = H; gray = C; red = O; blue = N.

The HOMO orbital of caffeic acid is saturated around the conjugated C=C double bond system, while the LOMO orbital lies along the carbon skeleton. Interestingly, both orbitals are similarly aligned, which, when considered side by side the total electron density, implies that the entire molecular skeleton would participate in the adsorption process. The HOMO energy (E_{HOMO}), reflects the capacity of a molecule to donate electrons, whereas the LUMO energy (E_{LUMO}) corresponds to a tendency for electron acceptance [39-42]. The HOMO/LUMO energy gap (ΔE) for caffeic acid was derived from the values E_{HOMO} = (-5.35 eV) and E_{LUMO} (-2.66 Ev) to be 2.69 eV. Low values of ΔE imply that minimal energy will be required to remove an electron from the last occupied orbital, corresponding to an increase in metal/inhibitor chemisorptive (covalent) interactions, hence improved inhibition efficiencies. Comparing the results from this study with that computed previously for caffeine [33] raises a number of interesting issues. The ΔE value for caffeic acid is lower than that for caffeine (3.57 eV), thus we expect caffeic acid to have better inhibition efficiency. However, the reverse was the case; caffeine exerted better inhibition efficiency (92.2%) than caffeic acid (84.3%) on copper corrosion in 10 % ethanolic 0.5 M NaCl.

In order to further explain the above findings, the non-covalent adsorption of the caffeic acid molecule on the Cu surface was visualized at a molecular level by means of molecular dynamics simulations. Typical snapshots of the lowest energy adsorption model for a single caffeic acid molecule on the Cu (110) surface are illustrated in Figure 11. In agreement with the electronic structure predictions, caffeic acid maintained a flat-lying alignment on the Cu surface.
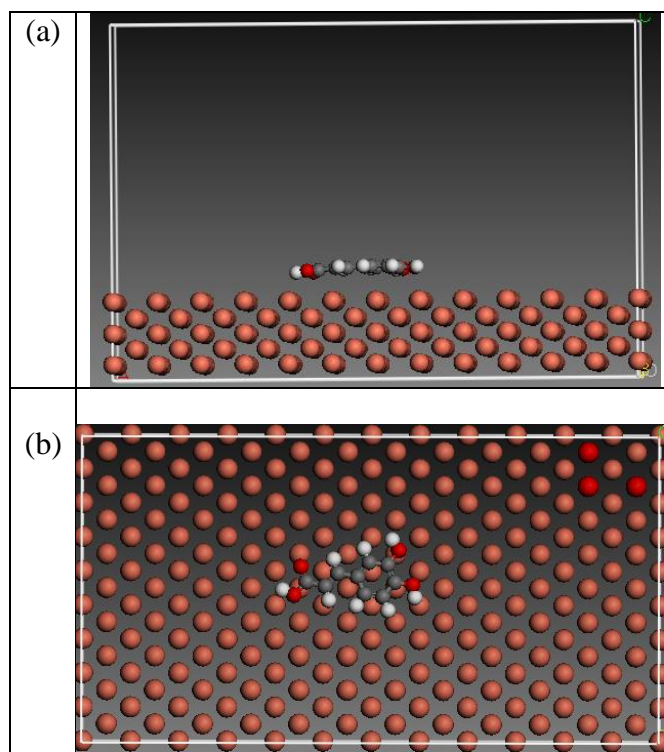
Figure 11. Molecular dynamics model of caffeic acid adsorbed on Cu (110): (a) side view; (b) on-top view

The binding energy (E_{Bind}) between each molecule and the Fe surface was calculated using Equation 11. E_{CA} is the energy of the caffeic acid molecule, E_{Cu} the energy of the Cu slab and E_{total} the energy of the caffeic acid/Cu(110) couple in the gas phase. The potential energies were obtained from mean values of the five structures with the lowest energy [42].

$$E_{Bind} = E_{total} - (E_{CA} + E_{Cu}) \qquad (11)$$

The obtained E_{Bind} value was - 44.14 kcal/mol. A direct correlation has been established between inhibition efficiency and binding energy, with efficiency increasing with binding energy [43]. This however should be mainly valid for systems exhibiting pronounced non-covalent interactions. The higher value of E_{Bind} for caffeine [33], with higher ΔE (which signify pronounced non-covalent interactions) corroborates this point of view.

4. CONCLUSIONS

The results of the electrochemical measurements have shown that caffeic acid acts as cathodic corrosion inhibitor for Cu in 10 % ethanolic 0.5 mol dm^{-3} NaCl solution.

The inhibition efficiency increases with the increase in caffeic acid concentration but decreases with the increase in temperature of the electrolyte.

The adsorption of organic compound on the Cu surface in 10 % ethanolic 0.5 mol dm^{-3} NaCl solution obeys the Freundlich adsorption isotherm model, and the calculated standard energy of adsorption suggest physical adsorption.

DFT-based quantum chemical computations provided mechanistic insights on the adsorption process and confirmed the spontaneous adsorption of caffeic acid on the Cu, with the caffeic acid molecule maintaining a flat-lying orientation on the surface.

References

1. H. Otmačić Čurković, E. Stupnišek-Lisac, H. Takenouti, *Corros. Sci.,* 52 (2010) 398-405.
2. D. A. Jones, Principles and Prevention of Corrosion, Macmillan, New York, 1992.
3. M. G. Fontana, Corrosion Engineering, third ed., McGraw-Hill, Singapore, 1986.
4. E. E. Oguzie, K. L. Iyeh, A. I. Onuchukwu, *Bull. Electrochem.,* 22 (2006) 63-68.
5. P. B. Raja, G. Sethuraman, *Matt. Lett.,* 62 (2008) 113-116.
6. M. Sangeetha, S. Rajendran, T.S. Muthumegala, A. Krishnaveni, *Zaštita materijala,* 52 (2011) 3-19.
7. A. M. Shah, A. A. Rahim, S. A. Hamid, S. Yahya, *Int. J. Electrochem. Sci.*, 8 (2013) 2140 -2153.
8. M. B. Petrović Mihajlović, M. M. Antonijević, *Int. J. Electrochem. Sci.*, 10 (2015) 1027-1053.
9. J. Sochor, O. Zitka, H. Skutkova, D. Pavlik, P. Babula, B. Krska, A. Horna, V. Adam, I. Provaznik, R. Kizek, *Molecules,* 15 (2010) 6285–6305.
10. T. Sun, P. W. Simon, S. A. Tanumihardjo, *J. Agric. Food Chem.,* 57 (2009) 4142–4147.
11. I. Gulcin, *Toxicology,* 217 (2006) 213-220.
12. S. Tsai, C. Chao, M. Yin, *European Journal of Pharmacology,* 670 (2011) 441–447.
13. I. Medina, I. Undeland, K. Larsson, I. Storro, T. Rustad, C. Jacobsen,V. Kristinova, J. M. Gallardo, *Food Chem.,* 131 (2012) 730-740.
14. L. Vrsalović, M. Kliškić, J. Radošević, S. Gudić, *J. Appl. Electrochem.,* 37 (2007) 325-330.
15. L. Vrsalović**,** M. Kliškić, S. Gudić, *Int. J. Electrochem. Sci.,* 4 (2009) 1568-1582
16. L. Vrsalović, E. Oguzie, M. Kliškić, S. Gudić, *Chem. Eng. Comm.*, 198 (2011) 1380-1393.
17. L. Narvaez, E. Cano, D. M. Bastidas, *J. Appl. Electrochem.*, 35 (2005) 499–506.
18. L. Pirvu, A. Armatu, C. Bubueanu, G. Pintilie, S. Nita, *Rom. Biotech. Lett.,* 15 (2010) 5683-5689.
19. L. Pirvu, D. Barbulescu, C. Nichita, S. Nita, S. C. Mihul, *Rom. Biotech. Lett.,* 16 (2011) 5937-5943.
20. F. S. de Sousa, A. Spinelli, *Corros. Sci.,* 51 (2009) 642-649.
21. E. McCafferty, D. C. Hansen, Proceedings of the 124th TMS Annual Meeting, Las Vegas, USA, Minerals, Metals & Materials Soc., (1995) 183-199.
22. I. Sekine, R. Komura, M. Yuasa, T. Wake, H. Murata, S. Someya, J. Udagawa, *Hyomen Gijutsu*, 50 (1999) 751-757.
23. M. Yuasa, K. Tokoro, T. Nakagwa, I. Sekine, T. Lamahama, Y. Shibata, T. Wake, *Hyomen \ Gijutsu,* 51 (2000) 524-529.
24. T. Szauer, A. Brandt, *Electrochim. Acta,* 26 (1981) 1253-1256.
25. E. E. Oguzie, J. Li, Y. Liu, D. Chen, Y. Li, K. Yang, F. Wang, *Electrochim. Acta*, 55 (2010) \5028-5035
26. E. E. Oguzie, Y. Li, F. H. Wang, *J. Appl. Electrochem.,* 37 (2007) 1183-1190
27. A. Popova, E. Sokolova, S. Raicheva, M. Christov, *Corros. Sci.,* 45 (2003) 33-58.
28. I. D. Raistrick, D. R. Franceschetti J. R. Macdonald, Theory, in: *Impedance Spectroscopy*, E. Barsoukov, J. R. Macdonald (Eds.), J. Wiley & Sons, Inc., New Jersey, 2005, pp. 27–128.
29. E. E. Oguzie, Z. O. Iheabunike, K. L. Oguzie, C. E. Ogukwe, M. A. Chidiebere, C. K.Enenebeaku, C. O. Akalezi, *J. Disper. Sci. & Tech.,* 34 (2013) 516-527.
30. H. Ma, S. Chen, L. Niu, S. Zhao, S. Li, *J. Appl. Electrochem.*, 32 (2002) 65–72.
31. E. Sherif, S.-M. Park*, J. Electrochem. Soc.*, 152 (2005) B428–B433.
32. C. O. Akalezi, C. K. Enenebeaku, E. E. Oguzie, *Inter. J. Ind. Chem.,* 3 (2012) 1-12

33. S. Gudić, E. E. Oguzie, A. Radonić, L. Vrsalović, I. Smoljko, M. Kliškić, *MJCCE*, 33 (2014)13-25.
34. E. Sherif, S.-M. Park, *Electrochim. Acta*, 51 (2006) 4665–4673.
35. K. F. Khaled, *Mater. Chem. Phys*., 112 (2008) 104–111.
36. E. E. Oguzie, B. N. Okolue, C. E. Ogukwe, C. Unaegbu, *Mater. Lett.,* 60 (2006) 3376-3378
37. L. Marıa Rodrıguez-Valdez, W. Villamisar, M. Casales, J.G. Gonzalez-Rodriguez, A.Martınez-Villafane, L. Martinez, D. Glossman-Mitnik, *Corros. Sci.,* 48 (2006) 4053-4064.
38. E. E. Oguzie, C. B. Adindu, C. K. Enenebeaku, C. E. Ogukwe, M. A. Chidiebere, K. L. Oguzie, *J. Phys. Chem. C*, 116 (2012) 13603-13615.
39. K. F. Khaled, K. Babic-Samardzija, N. Hackerman, *Electrochim. Acta*, 50 (2005) 2515-2520.
40. J. Cruz, E. Garcıa-Ochoa, M. Castro, *J. Electrochem. Soc.*, 150 (2003) B26-B35.
41. J. M. Roque, T. Pandiyan, J. Cruz, E. Garcıa-Ochoa, *Corros. Sci.,* 50 (2008) 614-624.
42. E. E. Oguzie, K. L. Oguzie, C. O. Akalezi, I. O. Udeze, J. N. Ogbulie, V. O. Njoku, *ACS Sustainable Chemistry & Engineering*, 1 (2012) 214-225
43. J. Bartley, N. Huynh, S. E. Bottle, H. Flitt, T. Notoya, D.P. Schweinsberg, *Corros. Sci.*, 45 (2003) 81-96.